Theoretical Physics Division
University of Oulu
P.O. Box 3000
FIN-90014, University of Oulu,
Finland

Gravitational Lensing and Cusp Slope Value Limit for the Dark Matter Halos

Petri Mutka
University of Oulu, Finland
e-mail: Petri.Mutka@oulu.fi

UNIVERSITY of OULU
OULUN YLIOPISTO
1958 2008

1 Introduction

We have developed an analytical theory for axially symmetric lensing with the GNFW profile (Navarro et al. 1996; Zhao 1996; Navarro et al. 1997). The density profile is strongly cusped at the center, i.e. when $r << 1$, density $\rho \propto r^{\alpha}$, where $\alpha = [-2, -1)$. We apply our theory to the statistical study of double-image quasar lenses.

The lensing model gives a relation between location of the optical axis, the cusp slope and the magnification ratio of the images. It does not depend directly on the cosmology, distances of the lens and the source nor mass of the lens object. We use this relation to derive statistics of the upper limits for the cusp slopes, which are capable producing observed magnification ratios for each lens. The composition of this distribution depends on the general properties of the lens dark matter halos (Mutka & Mähönen 2008).

The statistics is affected by several factors; the lens ellipticities (or other deviations from the axial symmetry), differential extinction, the variability of the source coupled to the time delay effects and the microlensing/perturbations by the substructure within the lens. Here we study the effects of the substructure on the overall statistics of the cusp slope limits (CSL) by creating mock lens catalogues with magnification perturbations.

2 The lens equation

The lens equation produced by a GNFW halo with cusp slope $\alpha = [-2, -1)$ becomes particularly simple when it is normalized with the Einstein radius of the lens (Mutka & Mähönen 2006):

$$l = \begin{cases} qk(1-|k|^{\alpha+1}) & k \le k_B \\ k - \frac{\alpha+1}{\alpha+3}\frac{k_B^2}{k}(1-q) & k > k_B \end{cases} . \qquad (1)$$

Here k is radial coordinate at the lens plane and l corresponding coordinate at the source plane. Information on the cosmology, lens and source distances, the mass and concentration of the lens object is embedded in the constant q.

The lens equation (1) has a piecewise definition, that is divided at

$$k_B = \left(\frac{2(q-1)}{q(\alpha+3)}\right)^{1/(\alpha+1)} \qquad (2)$$

in order to avoid negative surface densities. Because $q > 1$ by it's definition (Mutka & Mähönen 2006), it is easy to see that $k_B > (2/(\alpha+3))^{1/(\alpha+1)} > k_{cr1}$ always. Thence the maximum source coordinate l_{max} for strong lensing can be solved by setting $k = k_{cr1} = (\alpha+2)^{-1/(\alpha+1)}$ in the lens equation (1). See figure 1.

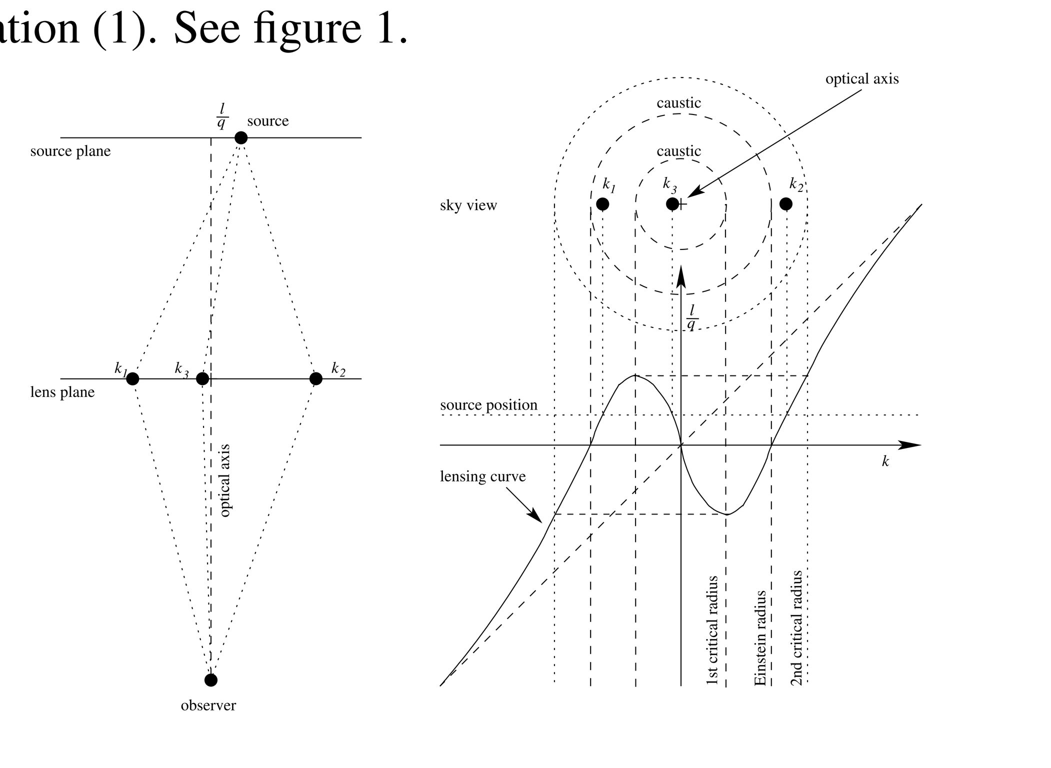

Figure 1: If the source coordinate $|l| < l_{max}$, axially symmetric lens produces three images at coordinates k_1, k_2 and k_3 according to the equation (1). The image at k_3 is usually strongly demagnified, thus most of the axially symmetric lens systems produce only two visible images.

3 The CSL analysis

Magnification of the images, cumulative mass function, convergence and shear of the lens can be acquired from the lens equation (1) as well. In general, for strong lensing it holds

$$\frac{|k_1|^{\alpha+2} + |k_2|^{\alpha+2}}{|k_1| + |k_2|} = 1, \qquad (3)$$

for the solutions of images k_1 and k_2 when $k < k_B$. Equation (3) holds most of the time, and it is broken only with large lens masses or concentrations when k_1 or k_2 exceeds the value k_B. With the lens equation (1) and relation (3) the magnification ratio μ_1/μ_2 of the images k_1 and k_2 can be written as

$$M = \frac{\mu_1}{\mu_2} = \theta \frac{|\theta^{\alpha+2} + 1 - (1+\theta)(\alpha+2)|}{|\theta^{\alpha+2} + 1 - \theta^{\alpha+1}(1+\theta)(\alpha+2)|}. \qquad (4)$$

Note that constant q has vanished from this expression. It is also possible to parametrize the lens equation with coordinate ratio $\theta = k_1/k_2$.

A solution $\alpha = \alpha_{CSL}$ and $\theta = \theta_{CSL}$ for the following pair of equations

$$\begin{cases} \frac{dM}{d\theta} = 0 \\ M \; = M_0 \end{cases} \qquad (5)$$

gives a CSL limit for the lens system. Here M_0 is the measured magnification ratio of the lens system. The value α_{CSL} is the minimum amount of "cuspiness", i.e. the maximum value for α, that is needed to produce observed magnification ratio M_0 with any lensing geometry assuming axial symmetry. Remarkable property of the CSL-value is that no information about location of the mass center or optical axis of the lens system is required (Mutka & Mähönen 2008).

The statistics of the α_{CSL} values are constructed by assuming that the source images ($(l/q) < (l/q)_{max}$) are uniformly distributed at the source plane. If all the lens systems in the sample have the same universal cusp slope value, a distinctive exponential distribution of α_{CSL} values is produced, see figure 2. If the cusp slopes of the halos are randomly distributed in some range of values, this feature is destroyed.

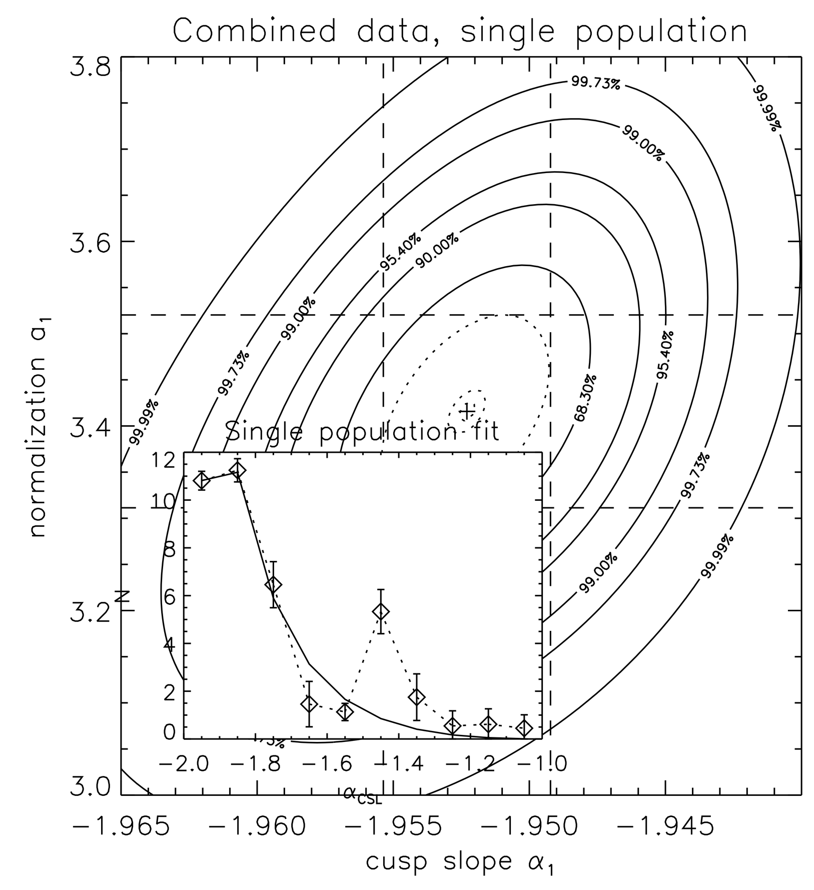

Figure 2: CSL-distribution for a sample of known double-image quasar lenses and the best fit for the distribution. The exponential slope in the observations is suggesting that there is a population of lenses with an universal cusp slope value $\alpha \sim -1.95$.

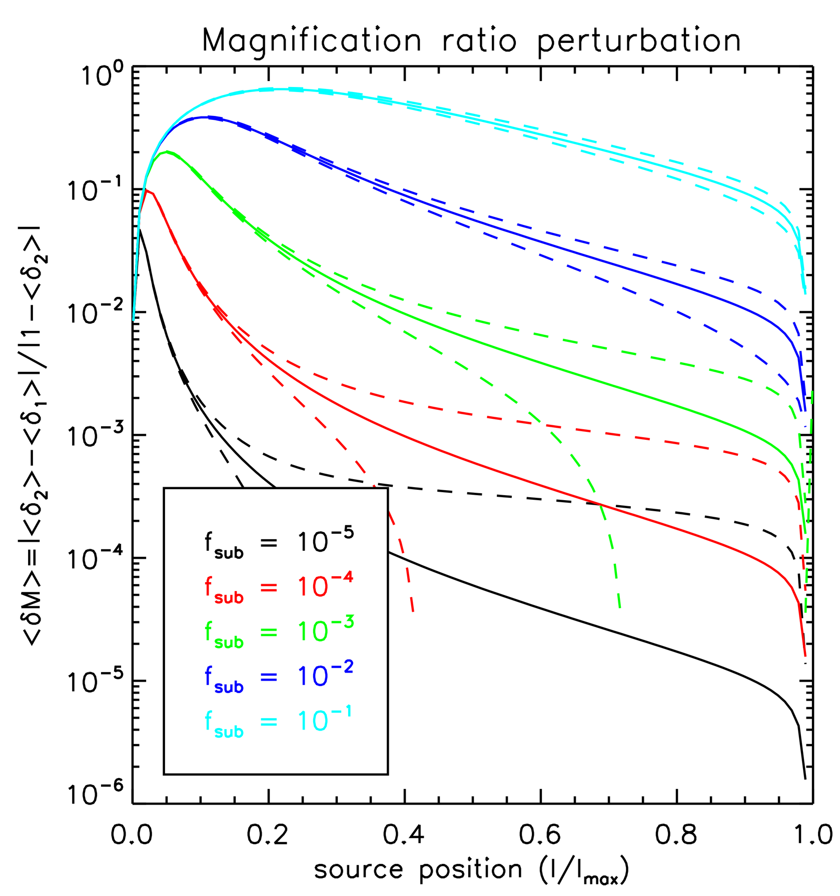

Figure 3: Expectation value $\langle \delta M \rangle$ for perturbations of the magnification ratio with different amounts of substructure f_{sub}. Corresponding dashed curves indicate standard deviation of the normal distribution ($z_l = 0.3$, $z_s = 1.5$, $M_l = 10^{12} M_{\odot}$).

4 Substructure

The effects of the substructure on the magnification of images is modelled with perturbations $\delta = \delta\mu/\mu$ that have normal distribution with expectation value $\langle\delta\rangle$ and variance var(δ). It is assumed that $|\delta| \ll 1$, thus the astrometric perturbations by the substructure is assumed being negligible, and only the changes in the fluxes of the images are considered. The moments of the distribution for the perturbations are calculated from the linear theory (Rozo et al. 2006).

Mass spectrum s of the SIS perturbers is assumed following $\mathrm{d}s/\mathrm{d}m \propto m^{\beta}$, where $\beta = -1.8$ (Gao et al. 2004). The amount of substructure is defined by ratio of substructure surface density to the critical density $f_{sub} = 2\Sigma_s/\Sigma_c$. The other parameter is the cutoff of the mass spectrum m_{max} that is chosen to be 1% of the virial mass of the lens object.

5 The synthetic lens catalogue

Effects of the substructure on the CSL analysis are studied by constructing mock lens catalogues. The Press-Schechter function is sampled at the suitable range for the lens and the source objects. The luminosity of the source object is related to the sampled mass for the source (Wyithe & Loeb 2002). The effects of the duty cycle time for the quasars on the luminosity function are ignored.

The magnification and image separation bias is introduced by solving the lens equation (1) for the system including the random perturbations by the substructure. The resulting lens system is accepted or rejected correspondingly if it exceeds the threshold magnitude and necessary image separation.

K-correction nor extinction need not to be accounted for, because we are using flux ratios of the images. The amount of substructure in the halos is studied by constructing multiple mock catalogues with varying degrees of strength for perturbations f_{sub}, and performing the CSL analysis.

6 Conclusions

The mock catalogues were produced with $\alpha = -1.95$, and the values were recovered through CSL analysis with moderate accuracy in all the cases. Strengthening the substructure seems to bring recovered value closer to the $\alpha = -2.0$, which corresponds to the SIS model for the macrolens.

The amount of substructure needed destroying the exponential distribution is clearly out of range of the linear perturbation theory. At the nonlinear regime the perturbers are affecting the overall convergence and shear of the lens thereby changing the macrolens solution as well, presenting a more challenging problem exceeding the scope of this presentation.

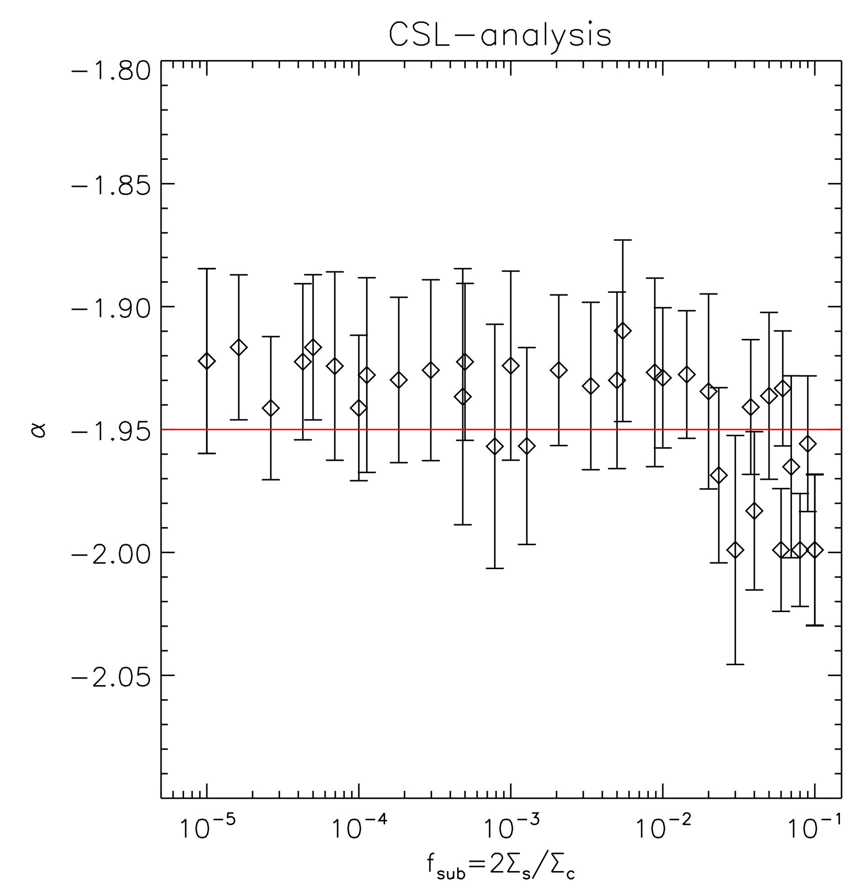

Figure 4: Recovered cusp slope values as a function of the substructure f_{sub} in the lenses. Each point represents a catalogue of 100 lens systems with $\alpha = -1.95$ (red line). Error bars represent 0.1 magnitude accuracy in the flux measurements and errors in fitting. Weighted mean of trials is $\alpha = -1.946 \pm 0.005$.

References

Mutka, P. T. & Mähönen, P. H., 2006, MNRAS, 373, 243.
Mutka, P. T. & Mähönen, P. H. 2008, manuscript in preparation.
Gao et al. ,2004 MNRAS, 355, 819.
Navarro, J. F., Frenk, C. S. & White, S. D. M. 1996, ApJ, 462, 563.
Navarro, J. F., Frenk, C. S. & White, S. D. M. 1997, ApJ, 490, 493.
Rozo, E., Zentner, A. R., Bertone, G. & Chen, J. 2006, ApJ, 639, 573.
Wyithe, J. S. B. & Loeb, A. L. 2002, ApJ, 581, 886.
Zhao, H. S. 1996, MNRAS, 278, 488.